Molecular Dynamics Simulations of the Hydrated Trivalent Transition Metal Ions Ti^{3+}, Cr^{3+}, and Co^{3+}

Chinapong Kritayakornupong, Jorge Iglesias Yagüe, and Bernd M. Rode*

Department of Theoretical Chemistry, Institute of General, Inorganic and Theoretical Chemistry, University of Innsbruck, A-6020 Innsbruck, Austria

Received: April 17, 2002; In Final Form: August 30, 2002

Molecular dynamics (MD) simulations based on ab initio evaluated two- and three-body potentials were performed for Ti^{3+}, Cr^{3+}, and Co^{3+} ions in water. The ions' hydration structure was evaluated in terms of radial distribution functions, coordination numbers, and angular distributions. The first solvation shell shows an exact coordination number of 6 for all ions and average $M^{3+}-O$ distances of 2.08, 2.05, and 2.03 Å for Ti^{3+}, Cr^{3+}, and Co^{3+}, respectively. The structural parameters obtained after inclusion of three-body correction terms are in good agreement with experimental values. The energies of hydration obtained from three-body corrected molecular dynamics simulations are also in good agreement with experiment, except for Ti^{3+} where the classical simulations are failing to reproduce the Jahn−Teller effect.

1. Introduction

In experiment, the Cr^{3+} ion is very stable in solution,[1] whereas Ti^{3+} easily oxidizes and its structure could be verified, therefore, only in the solid state.[2] Tachikawa et al.[3] have in addition carried out electron spin resonance (ESR), electron nuclear double resonance (ENDOR) and electron spin−echo studies to determine the hydration structure of Ti^{3+} ion in the amorphous solid of a 2-propanol/D_2O mixture, with the result that six water molecules coordinate to the central metal ion with an average $Ti^{3+}-O$ distance of 2.2 Å. The hexaquo Ti^{3+} ion persists in the solid-state structure of $TiCl_3 \cdot 6H_2O$[4] and the cesium alum $CsTi(SO_4)_2 \cdot 12H_2O$,[5] in which the $Ti^{3+}-O$ distance is quoted as 2.03 Å. The X-ray crystal structure of the pts^- ($C_7H_7O_3S^-$) salt $[Ti(OH_2)_6](pts)_3 \cdot 3H_2O$ has also been reported.[6] Here the geometry around Ti^{3+} was found to be essentially octahedral with Ti−O bond lengths ranging from 2.018 to 2.046 Å.

The hydration of Cr^{3+} has been the focus of many experimental[1,7−16] and theoretical[1,17−21] investigations and the ion was reported to have a kinetically extremely inert first coordination shell with six octahedrally coordinated water molecules,[1] using X-ray (XD),[1,7−9] neutron diffraction (ND),[1,10,11] LAXS,[13,14] and EXAFS methods.[1,14−16] The fact that it possesses a very stable first hydration shell has also presented a good opportunity to study the second hydration shell.[12−21] To our knowledge, only the second hydration shell structure has been studied by simulations, and no attempt has been made to study the first hydration shell of Cr^{3+} using statistical simulation methods. The highly oxidizing blue $[Co(H_2O)_6^{3+}]$ ion has been identified in alums[22,23] and in the hydrated sulfate $Co_2(SO_4)_3 \cdot 18H_2O$.[24]

The two- plus three-body interaction potential-based molecular dynamics (MD) simulations of this work were performed for systems consisting of M^{3+} (M = Ti, Cr, and Co) and 499 water molecules. The necessary potential functions were constructed from ab initio calculated energy surfaces at the Hartree−Fock level.

* Corresponding author. E-mail: Bernd.M.Rode@uibk.ac.at.

2. Details of Calculations

2.1. Selection of Basis Set. Obtaining appropriate basis sets for transition metal ion/water interactions, especially for trivalent metal ions, is a somewhat difficult task due to charge-transfer effects[25] resulting in M^{2+} and $(H_2O)^+$ species and thus erroneous energies at larger $M^{3+}-H_2O$ distances. Various combinations of full basis sets for metal and water have been tested to obtain basis sets suppressing this (gas phase) charge-transfer effect, but without result. Hence, to overcome this effect for the construction of M^{3+}/H_2O energy surfaces the original basis sets, which are optimized for neutral atoms, had to be modified to describe more appropriately the M^{3+} ions, which are much more contracted than the corresponding neutral metals.

2.1.1. $Ti^{3+}-H_2O$ Interaction. The ab initio effective core potentials (ECP) and double-ζ valence basis set developed by Stevens, Krauss, and Basch[26] were used omitting functions with exponents less than 0.5 and splitting the inner s and p orbitals to (5s5p4d)/[3s3p1d] for Ti^{3+}. For oxygen and hydrogen atoms, the DZV basis sets of Dunning were used.[27]

2.1.2. $Cr^{3+}-H_2O$ Interaction. For Cr^{3+}, the ab initio effective core potentials (ECP) basis set developed by LaJohn et al.,[28] omitting functions with exponents below 0.5, were used. For oxygen and hydrogen atoms, the 6-31G* basis sets of Pople et al. were employed.[29] The modification of the basis set for Cr^{3+} follows a previous work.[30]

2.1.3. $Co^{3+}-H_2O$ Interaction. The ab initio effective core potentials (ECP) basis set developed by LaJohn et al.,[28] omitting functions with exponents below 0.5, was used. For oxygen and hydrogen atoms, the 6-31G* basis sets of Pople et al. were employed.[29]

In all cases the ECP functions remained unchanged. Using the modified basis sets it was possible to calculate SCF energy points for the complete energy surfaces without artificial charge-transfer effects. Omitting the "soft" functions ($\alpha < 0.5$) appears an adequate tool to take into account the ionic radii of the M^{3+} ions, which are much smaller than the atomic radii of the corresponding neutral metal atoms.

The global minimum energies (at $\Theta = \phi = 0$, see Figure 1) of Ti^{3+}, Cr^{3+}, and Co^{3+} water complexes obtained with the

10.1021/jp020997n CCC: $22.00
Published on Web 10/15/2002

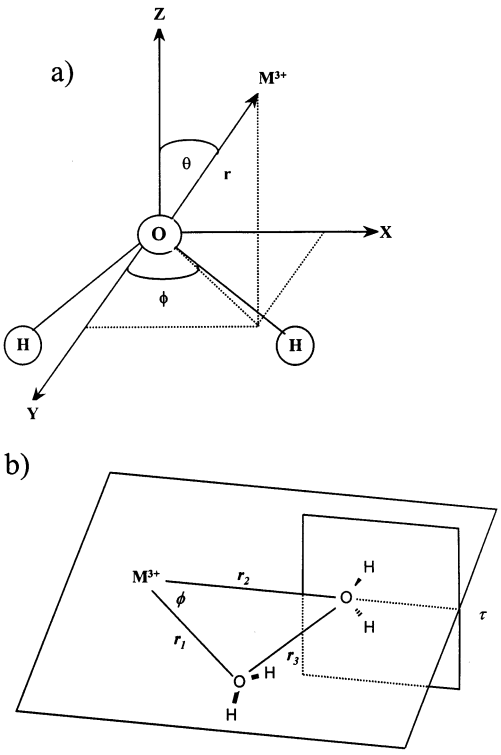

Figure 1. (a) Definition of geometric variables for M^{3+}−water orientations, H_2O molecules in *yz* plane. (b) Geometrical variations in SCF calculations on the $H_2O-M^{3+}-H_2O$ energy surfaces.

original basis sets are slightly higher than the minimum energies resulting from the modified basis sets. The distances $Ti^{3+}-H_2O$ and $Cr^{3+}-H_2O$ obtained with the modified basis sets are 0.01 Å shorter than those of the original basis sets, whereas the distance $Co^{3+}-H_2O$ remained unchanged. Since the calculations were performed to construct pair potential functions for simulations, the modest increase in energy could be tolerated, as the absolute energy values do not play such an important role for the evaluation of structural properties. The changes in $M^{3+}-O$ distances obtained by the modified basis sets are not significant. All SCF calculations were performed at the UHF level using the TURBOMOLE[31] program.

2.2. Construction of Two- and Three-Body Potentials. *2.2.1. Two-Body Potential.* To construct the $M^{3+}-H_2O$ pair potentials, the water was fixed in the origin of the coordinate system and the M^{3+} ion was moved in configuration space to numerous positions around the water molecule by varying geometrical parameters $0° \le \theta \le 180°$ and $0° \le \phi \le 90°$; for each configuration, the $M^{3+}-O$ inter-nuclear distances r were varied from 1.4 to 12.0 Å (Figure 1). The internal geometric parameters of water were held fixed at the experimental values,[32] i.e., $r_{OH} = 0.957$ Å and $\angle HOH = 104.5°$.

The interaction energies, ΔE_{2bd}, between water and an ion were evaluated by subtracting the ab initio energies of the isolated species $E_{M^{3+}}$ and E_{H_2O} from those of the monohydrates $E_{M(H_2O)^{3+}}$:

$$\Delta E_{2bd} = E_{M(H_2O)^{3+}} - E_{M^{3+}} - E_{H_2O} \quad (1)$$

For a representative description of the $M^{3+}-H_2O$ system, a total of 2000 energy points for the monohydrates were generated. Subsequently, fittings were performed with various potential types appropriate to describe electrostatic and van der Waals interactions as well.

2.2.2. Three-Body Corrections. $H_2O-M^{3+}-H_2O$ configurations were generated by independently varying both $M^{3+}-O$ distances ($1.8 \le r_{M^{3+}-O} \le 6.0$ Å) r_1 and r_2, the distance O−O between water molecules, r_3, and the torsional angle ($\tau = 0°$, 45°, and 90°) between the planes of the two ligands as shown in Figure 1. The three-body interaction energy ΔE_{3bd} for each configuration was evaluated by subtracting the two-body energies ΔE_{2bd} of $M^{3+}-$water and water−water[33] interactions as follows:

$$\Delta E_{3bd} = E_{M(H_2O)_2^{3+}} - E_{M^{3+}} - 2E_{H_2O} - \Delta E_{2bd}(M^{3+} - H_2O)_1 - \Delta E_{2bd}(M^{3+} - H_2O)_2 - \Delta E_{2bd}(H_2O - H_2O) \quad (2)$$

For each system (Ti^{3+}, $Cr^{3}+$, or Co^{3+}) a total of 6000 configurations were generated in the configuration space around M^{3+}, using the same basis set as in the construction of the pair potentials.

2.3. MD Simulations. *2.3.1. Pair Potential.* The MD simulations were carried out for systems consisting of one M^{3+} ion and 499 water molecules in a periodic cube at the temperature 298.16 K. The density of 0.997 g cm^{-3} was assumed to be the same as that of pure water. A radial cutoff limit of half the box length (12.345 Å) for Coulombic and non-Coulombic terms was chosen with the exception of non-Coulombic O−H and H−H interactions where a cutoff of 5 and 3 Å, respectively, was sufficient. In addition, a reaction field[34] was established to properly account for long-term Coulombic interactions. For water−water interactions the flexible BJH-CF2 model was used[33] and as this flexible CF2[35] water model allows explicit hydrogen movements, the time step was chosen as 0.2 fs. The CF2 model was chosen, as it is more consistent with our type of ion−water potential[36] than the MCY,[37] and in contrast to rigid models[38] (TIP3P, TIP4P, and TIP5P) allows an adaptation of HOH angle and OH bond length in the ligand molecules upon complexing the metal ion.

The water box, subject to periodic boundary conditions, was equilibrated for 100 000 time steps in the NVT-ensemble. To maintain a constant temperature of 298.16 K a temperature scaling algorithm[39] with a relaxation time of $\tau = 0.1$ ps was applied along the whole simulation. A further 400 000 steps of MD simulation were carried out under the same conditions as the equilibration, to provide data for structural evaluation.

2.3.2. Inclusion of Three-Body Corrections. The MD simulations, this time including three-body corrections, have been carried out. Under the same conditions as in 2.3(a), the starting configuration of the water box was taken from the MD simulation using only pair potentials, and 100 000 time steps in the NVT-ensemble were needed for equilibration. A further 800 000 time steps provided the data for sampling.

3. Results and Discussion

3.1. Two- and Three-Body Potentials. *3.1.1. Pair Potential.* Fitting of the pair interaction energies for $M^{3+}-H_2O$ interactions to a functional form was performed by the least-squares method with Levenberg-Marquart algorithm. After testing various potential types in order to describe all electrostatic and Van der Waals interactions, the best functions resulted as

$$\Delta E_{FIT} = \sum_i (A_{iM} r_{iM}^{-a} + B_{iM} r_{iM}^{-b} + C_{iM} r_{iM}^{-c} + D_{iM} r_{iM}^{-d} + q_i q_M r_{iM}^{-1}) \quad (3)$$

where A_{iM}, B_{iM}, C_{iM}, and D_{iM} are fitting parameters, r_{iM} are the distances between the ith atom of H_2O and M^{3+}, q_i are the

TABLE 1: Final Optimized Parameters of Pair Potential and Three-Body Correction Functions for M^{3+}−Water (M = Ti^{3+}, Cr^{3+}, or Co^{3+}) Interactions[a]

2-Body

pair	A (kcal mol^{-1})	B (kcal mol^{-1})	C (kcal mol^{-1})	D (kcal mol^{-1})
Ti^{3+}−O	−6998.6692598 Å^4	27955.4490615 Å^6	−29711.3491460 Å^8	11460.9827625 Å^{12}
Ti^{3+}−H	2106.3850842 Å^4	−6501.7401192 Å^6	5764.1175382 Å^8	
Cr^{3+}−O	−7657.0142355 Å^5	97017.2198911 Å^8	−110764.5391522 Å^9	17811.9667684 Å^{12}
Cr^{3+}−H	198.3423800 Å^5	−957.4655702 Å^8	869.2803874 Å^{12}	
Co^{3+}−O	−7937.7165312 Å^5	126798.3728493 Å^8	−167197.13403 Å^9	60178.0564410 Å^{12}
Co^{3+}−H	632.3681017 Å^5	−3542.2821515 Å^8	3102.9356913 Å^9	115.8742531 Å^{12}

3-Body

H_2O−M^{3+}−H_2O	A_1 (kcal mol^{-1} Å^{-4})	A_2 (Å^{-1})	A_3 (Å^{-1})
Ti^{3+}	0.0639943	−0.2179482	0.3053575
Cr^{3+}	0.8727987	0.2593399	0.5041385
Co^{3+}	0.6560400	0.3284183	0.4201692

[a] Charges on O and H, taken from the CF2[33] water−water interaction potential, are −0.6598 and 0.3299, respectively. Final optimized parameters of pair potential and three-body correction functions for Cr^{3+} interactions was taken from the previous work in our group.[30]

atomic net charges of the ith atom of H_2O, q_M is the atomic net charge of M^{3+}, and a, b, c, and d are exponents. Similar analytical potential functions have been successfully used for other hydrated metal ions.[40,41] The final parameters of the functions are given in Table 1.

3.1.2. Three-Body Corrections. The resulting three-body corrections obtained for each system under study were fitted to the following functional form to be added to the pair potentials

$$\Delta E_{3bd} = A_1 \exp(-A_2 r_{M^{3+}-O_1}) \exp(-A_2 r_{M^{3+}-O_2}) \exp(-A_3 r_{O_1-O_2}) \times [(CL - r_{M^{3+}-O_1})^2 \times (CL - r_{M^{3+}-O_2})^2] \quad (4)$$

where A_n are fitting parameters, o_i refer to the center of mass of the water molecules, and CL represents the cutoff limit set to 6.0 Å, the maximum distance to which three-body corrections were evaluated, because nonadditive contributions at farther distances were of no significance. The chosen analytical function ensures that ΔE_{3bd} becomes zero at the cutoff limit and gives a steady transition into the region where only the pair potential function is used. The final parameters of the three-body correction functions for H_2O−M^{3+}−H_2O are shown in Table 1.

3.2. Structural Data. *3.2.1. Pair Potential Simulations.* The results obtained from MD simulations with only pair potential are far from realistic values. The average first hydration shell coordination numbers are overestimated, 9 for Ti^{3+} and 8 for Cr^{3+} and Co^{3+} ions, respectively. The M^{3+}−O RDFs show small additional peaks that are known as an artifact of simulations with only pair potentials.[42] The angular distributions obtained show unusual ligand orientations due to the presence of too many water molecules in the first hydration shells of Ti^{3+}, Cr^{3+}, and Co^{3+} ion, respectively. It is obvious from these results that simulations based on ab initio pair potentials are, as expected, inadequate to determine coordination numbers and thus even a rough structure of hydrated trivalent ions, and that at least three-body correction is mandatory to describe the hydration of these ions.

3.2.2.1. Ti^{3+}−H_2O. The Ti^{3+}−O and Ti^{3+}−H RDFs obtained after inclusion of three-body effects from MD simulation are shown in Figure 2. The Ti^{3+}−O RDF obtained from MD simulations shows three peaks. The first peak in the Ti^{3+}−O RDF, which corresponds to the first hydration shell, is centered at 2.08 Å, the second-shell peak is centered 4.77 Å. This implies that the first hydration shell is well separated from the second hydration shell. In the Ti^{3+}−O RDF, a third peak centered at 5.84 Å is observed. This splitting of the second shell has also been observed in the case of Fe^{3+},[30] but not in our simulation of Cr^{3+} and Co^{3+}. It seems to be a phenomenon associated with these types of ions and will be subject of simulations with more refined techniques.

TABLE 2: Characteristic Values of the Radial Distribution Functions, $g_{\alpha\beta}(r)$, for Ti^{3+}, Cr^{3+}, and Co^{3+} in Water Determined by Molecular Simulation Methods[a]

$\alpha-\beta$	r_{M1}	r_{m1}	n_1	r_{M2}	r_{m2}	n_2
Ti−O	2.08	2.30	6.00	4.77	5.24	11.17
Cr−O	2.05	2.37	6.00	4.45	5.25	18.28
Co−O	2.03	2.29	6.00	4.43	4.91	18.80

[a] r_{M1}, r_{M2} and r_{m1}, r_{m2} are the distances in Å, where $g_{\alpha\beta}(r)$ has the first and second maximum and the first and second minimum, respectively. n_1 and n_2 are the coordination numbers of the first and second shells, respectively.

Despite this splitting, the Ti^{3+}−H RDF shows only two peaks, the first peak being centered at 2.95 Å. This distance in relation to the corresponding oxygen RDF peak indicates that in the first shell the water molecules are clearly oriented to follow the dominant ion−water dipole interaction with the oxygen atoms pointing to the ion. Some characteristic values for Ti^{3+}−O radial distribution functions are listed in Table 2. Since the simulation performed does not include higher than three-body effects it cannot account for the Jahn−Teller effect[43] which is expected to occur in $[Ti(H_2O)_6]^{3+}$ but the Ti^{3+}−O distance appears to be a reasonable average of the results obtained in the solid state[5−7] (2.03 Å) and those obtained for the amorphous solid of a 2-propanol/D_2O mixture by Tachikawa,[4] 2.20 Å.

The most significant improvement over pair potential results is the change of the first hydration shell coordination to 6 (Figure 3). The mean coordination number for the second hydration shell results as 11.2 in the MD simulations, implying that every first-shell water molecule interacts with about 2 water molecules in the second shell. This shows that ligand orientation and binding should be almost entirely determined by hydrogen bonding.

The hydration shell structure of Ti^{3+} can be illustrated on the basis of O−Ti^{3+}−O angular distribution functions (Figure 4). The angular distributions display only two peaks centered at 90° and 175° in MD simulations, corresponding to a slightly distorted octahedral complex.

3.2.2.2. Cr^{3+}−H_2O. The resulting RDFs for Cr^{3+}−O and Cr^{3+}−H from the three-body corrected simulations are plotted in Figure 2. In the Cr^{3+}−O RDF, a sharp peak centered at 2.05

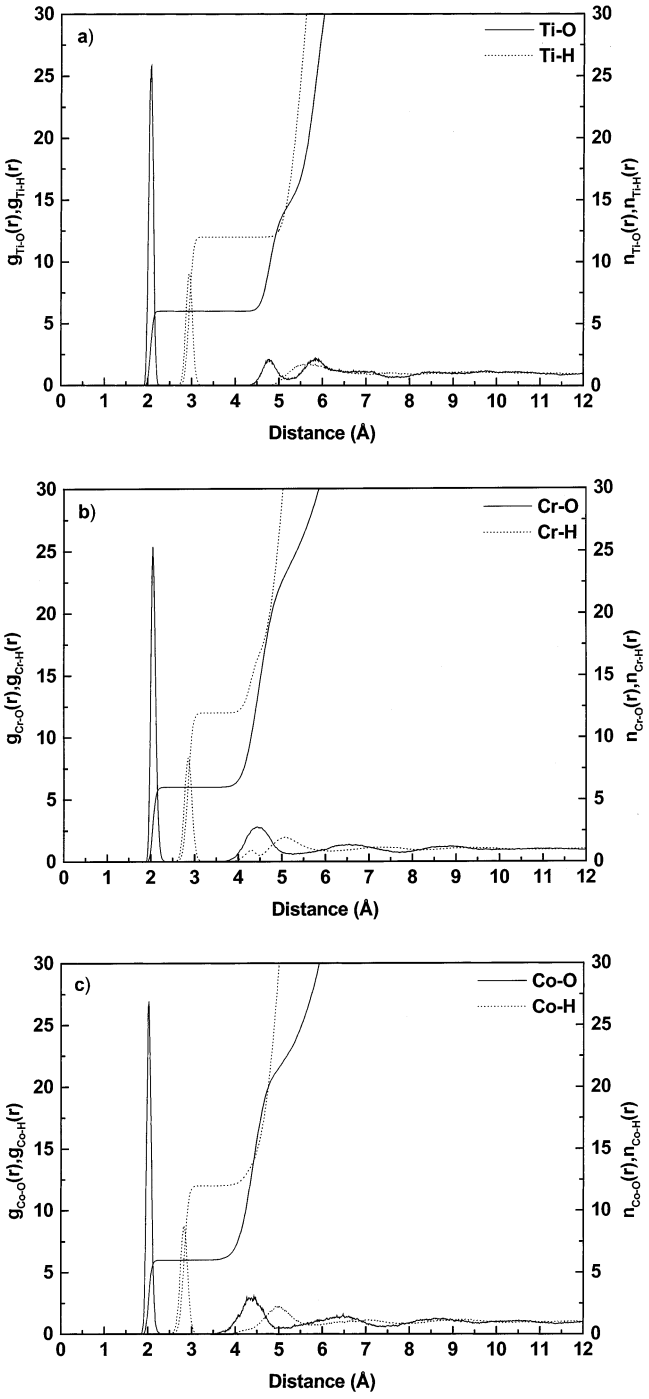

Figure 2. $M^{3+}-O$ and $M^{3+}-H$ (M = (a) Ti, (b) Cr, (c) Co) radial distribution functions and their running integration numbers obtained by MD simulations including three-body corrections.

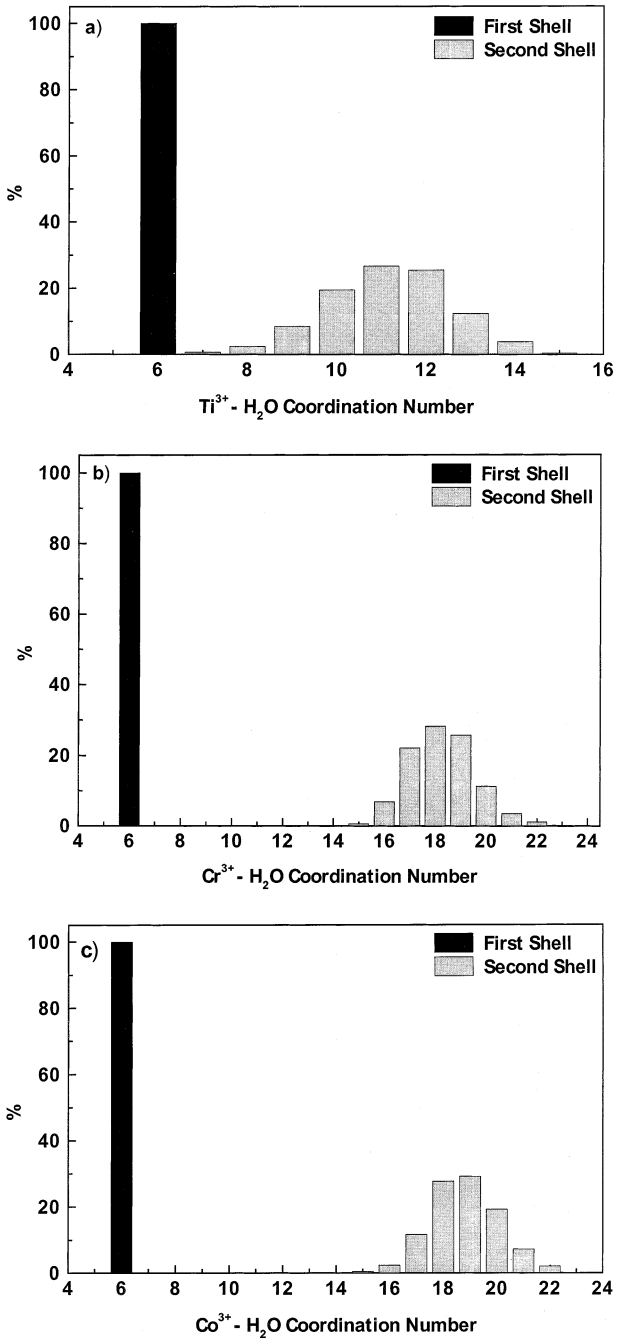

Figure 3. First- and second-shell coordination number distributions of hydrated M^{3+} (M = (a) Ti, (b) Cr, (c) Co) MD simulations including three-body corrections.

Å represents the first hydration shell. The $Cr^{3+}-O$ RDF further shows the presence of a well-defined second hydration shell centered at 4.45 Å, followed by a broad peak centered at ~6.5 Å. The latter could be ascribed to a diffuse third hydration shell and it reflects mainly the strong ordering effect induced on the solvent by the Cr^{3+} ion. The $Cr^{3+}-O$ RDF becomes zero after its first peak and remains almost zero for more than 1 Å, suggesting that the first hydration shell is very stable and that ligand exchange with the second shell must be rather marginal, in agreement with experimental results ($k(298) = 2.4 \times 10^{-6}$).[44]

The $Cr^{3+}-H$ RDF confirms the presence of first and second hydration shell by peaks centered at 2.85 and 5.09 Å, respectively. The distances of the $Cr^{3+}-H$ RDF peaks, 0.7 Å larger than those of the corresponding $Cr^{3+}-O$ RDF peaks, indicate that especially in the first shell, the water molecules are strictly oriented to point with oxygen to the ion and that the first shell has quite a rigid structure. The characteristic values for the $Cr^{3+}-O$ radial distribution function obtained by the three-body corrected MD simulation are listed in Table 2 and compared to other results in Table 3.

The mean coordination numbers of the first and second hydration shells of Cr^{3+} result as 6 and 18.3, respectively. Quite different coordination numbers for the second shell (12 and 14) have resulted from MC simulations using the MCY model for water.[18,20] The average Cr−O distance of the second shell obtained by EXAFS technique is 4.00 Å, a slightly longer distance (4.06−4.08 Å) was found by MC simulation. The rather high coordination number of 18 and the associated Cr−O

TABLE 3: Comparison of Hydration Structure Parameters for Cr^{3+}

solution	$\alpha-\beta$	N^a (concentrated)	$r_1{}^b$	$n_1{}^c$	$r_2{}^b$	$n_2{}^c$	method	ref
$CrCl_3$	Cr−O	1 M	1.994(3)	6	4.05(2)	12	XRD	7
$Cr(NO_3)$	Cr−O	1 M	1.999(3)	6	4.08(1)	12	XRD	7
		0.5 M	1.98	6	4.20−4.25		XRD	8
		0.05 m	2.00 ± 0.01	6.0 ± 0.1	3.97 ± 0.08	13.4 ± 1.3	EXAFS	14
		0.01 m	2.01 ± 0.01	6.0 ± 0.1	4.02 ± 0.08	13.4 ± 1.3	EXAFS	14
		0.001 m	2.01 ± 0.01	6.4 ± 0.1	4.00 ± 0.08	13.6 ± 1.0	EXAFS	14
$[Cr(H_2O)_6]^{3+}$	Cr−O	512			4.08	12.3 ± 0.01	MC	20
$[Cr(H_2O)_6]^{3+}$	Cr−O	512			4.06 ± 0.02	14 ± 1	MC	18
Cr^{3+}	Cr−O	499	2.05	6.0	4.45	18.28 ± 0.01	MD	this work

[a] Number of H_2O molecules in the simulation box. [b] r_i is the distance in Å of the *i*th maximum of the RDF. [c] n_i is the average hydration number integrated up r_{im} of the *ith* shell.

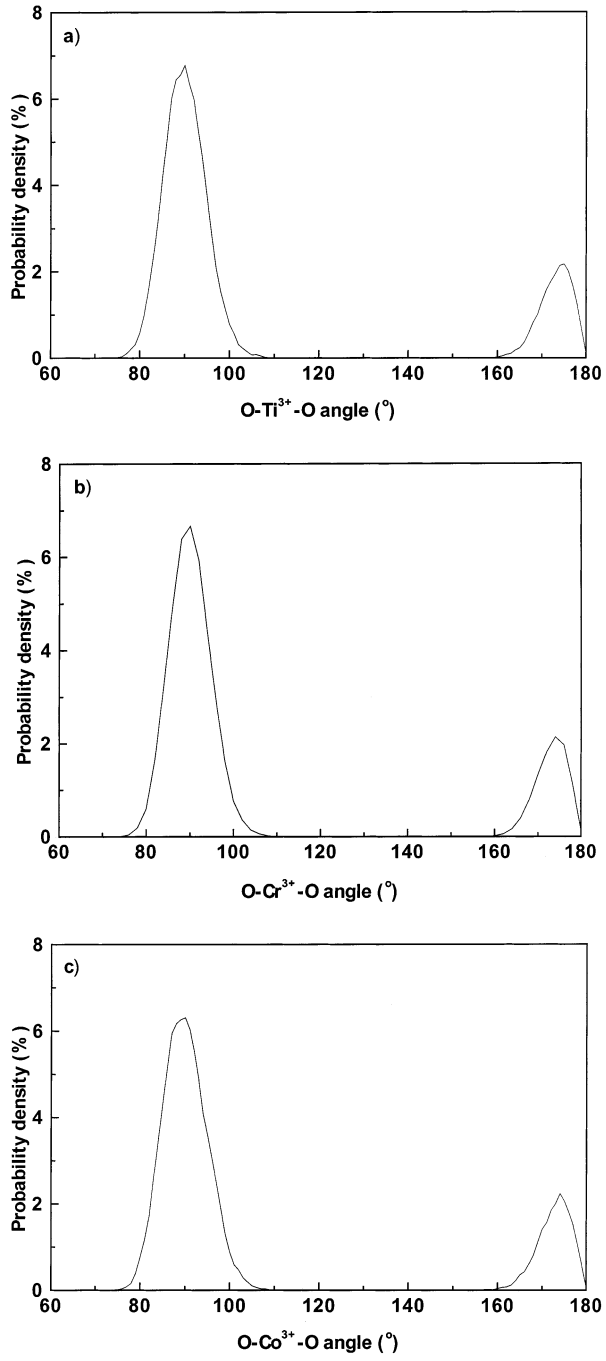

Figure 4. Distribution of the bond angles $H_2O-M^{3+}-H_2O$ (M = (a) Ti, (b) Cr, (c) Co) MD simulations including three-body corrections.

distance (4.45 Å) of the second shell resulting in our simulation may be related to the CF2 water model; it may also indicate, however, that the inclusion of three-body effects is not yet sufficient to obtain a good picture of the second shell.

In Figure 4, the $O-Cr^{3+}-O$ angular distribution calculated up to the first minimum of the $Cr^{3+}-O$ RDFs is shown. The angular distribution shows two peaks with maximum values at 90° and 174°, corresponding to the expected octahedral geometry.

3.2.2.3. Co^{3+}-H_2O. The $Co^{3+}-O$ and $Co^{3+}-H$ RDFs are shown in Figure 2. The first $Co^{3+}-O$ maximum peak is centered at 2.03 Å, a second peak is located around 4.43 Å. The first solvation shell is thus clearly separated from the second one, the coordination number is 6. The $Co^{3+}-H$ RDF peaks of the first and second hydration shell are centered at 2.83 and 4.97 Å, respectively. The characteristic values for $Co^{3+}-O$ radial distribution functions (RDFs) are also listed in Table 2.

The percentage distribution of coordination numbers of hydrated Co^{3+} ion in the first and second shell has also been analyzed and is shown in Figure 3. The mean coordination number of the first and second hydration shells result as 6 and 18.8, respectively, which indicates that every first-shell water molecule interacts with about 3 water molecules in the second shell.

The $O-Co^{3+}-O$ angular distribution calculated up to the first minimum of the $Co^{3+}-O$ RDF is shown in Figure 4, showing two peaks with maximum values at 90° and 174° corresponding to the expected octahedral geometry.

Finally, the hydration energies were evaluated for a comparison of simulation and experimental data. The absolute standard molar enthalpies of hydration obtained from TATB extrathermodynamic assumption,[45] which uses several salts with tetraphenyl-shielded ions for the evaluation of single-ion enthalpies at 298.15 K, were determined as −1038 kcal/mol, −1117 kcal/mol, and −1122 kcal/mol[45] for Ti^{3+}, Cr^{3+}, and Co^{3+}, respectively. The energies of hydration obtained from three-body-corrected molecular dynamics simulations are −1160 ± 16 kcal/mol, −1141 ± 13 kcal/mol, and −1163 ± 14 kcal/mol for Ti^{3+}, Cr^{3+}, and Co^{3+}, respectively. The hydration energies of Cr^{3+} and Co^{3+} are close to the experimentally estimated values, whereas the deviation is over 10% in the case of Ti^{3+}. This could be expected, however, as the well-known Jahn−Teller effect[43] occurring with Ti^{3+} is not accounted for by a classical molecular dynamics simulation, even with 3-body corrections.[46]

4. Conclusion

Ab initio two-body potentials are definitely inadequate to describe the hydration structure of Ti^{3+}, Cr^{3+}, and Co^{3+} ions. The inclusion of 3-body effects reduces the average first shell coordination numbers from 9 and 8 (pair potential values) to 6 for all M^{3+} ions. The results of this study, therefore, suggest that any successful simulation of triply charged transition metal

cations in aqueous solution must include at least three-body effects to give correct structural parameters. The first shell coordination numbers and ion−ligand distances thus obtained are in good agreement with experimental data. For the second hydrated shell, remarkable differences are observed for Ti^{3+} on one hand and for Co^{3+} and Cr^{3+} on the other. The appearance of a split second shell peak in the case of Ti^{3+} and disagreement of the average Cr^{3+}−O distance of the second shell between simulation and experiment suggest that polarization and charge-transfer effects of higher order have to be considered in the simulation. Thus, it seems desirable to include in further studies higher *N*-body effects as also needed to account for the Jahn−Teller effect, which occurs in $[Ti(H_2O)_6]^{3+}$ and has been observed in a QM/MM-MC simulation of hydrated Cu^{2+}.[46] The use of the much more computer time-consuming (factor of ∼100) quantum mechanics-based QM/MM technique also promises more accurate results for the second hydration shell of all 3 ions investigated here, and will thus be used in subsequent studies.

Acknowledgment. Financial support by The Austrian Science Foundation, Project No. P13644-TPH, and a scholarship of the Austrian Federal Ministry for Foreign Affairs for C.K are gratefully acknowledged.

References and Notes

(1) Ohtaki, H.; Radnai, T. *Chem. Rev.* **1993**, *93*, 1157.
(2) (a) Beattie, J. K.; Best, S. P.; Skelton, B. W.; White, A. H. *J. Chem. Soc., Dalton Trans*. **1981**, 2105. (b) Best, S. P.; Forsyth, J. B.; Tregenna-Piggott, P. L. *J. Chem. Soc., Dalton Trans*. **1993**, 2711.
(3) Tachikawa, H.; Ichikawa, T.; Yoshida, H. *J. Am. Chem. Soc.* **1990**, *112*, 977.
(4) Furman, S. C.; Garner, C. S. *J. Am. Chem. Soc.* **1951**, *73*, 4528.
(5) (a) Lipson, H. *Proc. R. Soc. London A* **1935**, *151*, 347. (b) Hartmann, H.; Schlafer, H. L. *Z. Naturforsch.* **1951**, *A6*, 754.
(6) Aquino, M. A. S.; Clegg, W.; Liu, Q. T.; Sykes, A. G. *Acta Cryst*. **1995**, *C51*, 560.
(7) Camaniti, R.; Licheri, G.; Piccagula, G.; Pinna, G. *J. Chem. Phys.* **1978**, *69*, 1.
(8) Bol, W.; Welzen, T. *Chem. Phys. Lett.* **1977**, *49*, 189.
(9) Magini, M. *J. Chem. Phys.* **1980**, *73*, 2499.
(10) Broadbent R. D.; Neislon, G. W.; Sandstörm M. *J. Phys.: Condens. Matter* **1992**, *4*, 639.
(11) Johansson, G. *Adv. Inorg. Chem*. **1992**, *39*, 159.
(12) Read, M. C.; Sandström, M. *Acta Chem. Scand.* **1992**, *46*, 1177.
(13) Lindqvist-Reis, P.; Muñoz-Páez, A.; Diáz-Moreno, S.; Pattanailk, S.; Persson, I.; Sandström, M. *Inorg. Chem.* **1998**, *37*, 6675.
(14) Muñoz-Páez, A.; Pappalardo, R. R.; Sánchez Markos, E. *J. Am. Chem. Soc.* **1995**, *117*, 11710.
(15) Sakane, H.; Muñoz-Páez, A.; Díaz-Moreno, S.; Martínez, J. M.; Pappalardo, R. R.; Sánchez Markos, E. *J. Am. Chem. Soc.* **1998**, *120*, 10401.
(16) Bieuzen, A.; Foglia, F.; Furet, E.; Helm, L.; Merbach, A. E.; Weber, J. *J. Am. Chem. Soc*. **1996**, *118*, 12777.
(17) Pappalardo, R. R.; Sánchez Markos, E. *J. Chem. Phys.* **1993**, *97*, 4500.
(18) Sánchez Markos, E.; Pappalardo, R. R.; Martínez, J. M. *J. Phys. Chem.* **1996**, *100*, 11748.
(19) Floris, F.; Persico, M.; Tani, A.; Tomasi, J. *Chem. Phys.* **1995**, *195*, 207.
(20) Martínez, J. M.; Hernández-Cobos, J.; Saint-Martin, H.; Pappalardo, R. R.; Sánchez Marcos, E. *J. Chem. Phys.* **2000**, *112*, 2339.
(21) Martínez, J. M.; Pappalardo, R. R.; Sánchez Marcos, E. *J. Chem. Phys.* **1998**, *109*, 1445.
(22) Figgis, B. N.; Lewis, J. *Prog. Inorg. Chem.* **1964**, *6*, 34.
(23) Bast, S. P.; Armstrong, R. D.; Beattie, J. K. *J. Chem. Soc., Dalton. Trans.* **1981**, 2105.
(24) Swann, S.; Xanthakos, T. S. *J. Am. Chem. Soc.* **1931**, *53*, 400.
(25) Corongiu, G.; Clementi, E. *J. Chem. Phys.* **1978**, *69*, 4885.
(26) Stevens, W. J.; Krauss, M.; Basch, H.; Jasien, P. G. *Can. J. Chem*. **1992**, *70*, 612.
(27) (a) Dunning, T. H.; Hay, P. J. In *Methods of Electronic Structure Theory*; Schaefer, H. F., III., Ed.; Plenum Press: New York, 1977; Vol. 3. (b) Dunning, T. H., Jr. *J. Chem. Phys.* **1970**, *53*, 2823.
(28) LaJohn, L. A.; Christiansen, P. A.; Ross, R. B.; Atashroo, T.; Ermler, W. C. *J. Chem. Phys.* **1987**, *87*, 2812.
(29) Hariharan, P. C.; Pople, J. A. *Theor. Chim. Acta* **1973**, *28*, 213.
(30) Mohammed, A. M. Molecular Simulation of Transition Metal in Aqueous Solution. Dissertation, University of Innsbruck, Austria, 2001.
(31) (a) Ahlrichs, R.; Bär, M.; Häser, M.; Horn, H.; Kölmel, C. *Chem. Phys. Lett.* **1989**, *162*, 165. (b) Brode, S.; Horn, H.; Ehrig, M.; Moldrup, D.; Rice, J. E.; Ahlrichs, R. *J. Comput. Chem.* **1993**, *14*, 1142. (c) von Arnim, M.; Ahlrichs, R. *J. Comput. Chem.* **1998**, *19*, 1746. (d) Ahlrichs, R.; von Arnim, M. In *Methods and Techniques in Computational Chemistry: METECC-95*; Clementi, E., Corongiu, G., Eds.; Club Européen MOTECC: Namur, Belgium, 1995; pp 509−554.
(32) Benedict, W. S.; Gailar, N.; Plyler, E. K. *J. Chem. Phys.* **1956**, *24*, 1139.
(33) Jancsó, G.; Heinzinger, K.; Bopp. P. *Z. Naturforsch.* **1985**, *A40*, 1235.
(34) Müller-Plathe, F. *Comput. Phys. Commun.* **1993**, *78*, 77.
(35) (a) Stillinger, F. H.; Rahman, A. *J. Chem. Phys.* **1978**, *68*, 666. (b) Jancsó, G.; Bopp, P.; Heinzinger, K. *Chem. Phys. Lett.* **1983**, *98*, 129.
(36) Rode, B. M. *J. Phys. Chem.* **1992**, *96*, 4170.
(37) Matsuoka, O.; Clementi, E.; Yoshimine, M. *J. Phys. Chem.* **1976**, *79*, 1351.
(38) Mahoney, M. W.; Jorgensen, W. L. *J. Chem. Phys.* **2000**, *112*, 8910.
(39) Berendsen, H. J. C.; Postma, J. P. M.; van Gunsteren, W. F.; DiNola, A.; Haak, J. R. *J. Chem. Phys.* **1984**, *81*, 3685.
(40) Marini, G. W.; Texler, N. R.; Rode, B. M. *J. Phys. Chem.* **1996**, *100*, 6808.
(41) Texler, N. R.; Rode, B. M. *J. Chem. Phys.* **1995**, *99*, 15714.
(42) Yagüe, J. I.; Mohammed, A. M.; Loeffler, H.; Rode, B. M. *J. Phys. Chem. A* **2001**, *105*, 7646.
(43) Jahn, H. A.; Teller, E. *Proc. R. Soc. London A* **1937**, *161*, 220.
(44) Helm, L.; Merbach, A. E. *Coord. Chem. Rev.* **1999**, *187*, 151.
(45) Marcus, Y. *J. Chem. Soc., Faraday Trans.* **1987**, *83*, 339.
(46) Marini, G. W.; Liedl, K. R.; Rode, B. M. *J. Phys. Chem. A* **1999**, *103*, 11387.